Available online on 15.11.2025 at http://jddtonline.info

Journal of Drug Delivery and Therapeutics

Open Access to Pharmaceutical and Medical Research



*Open Access Full Text Article*

Research Article

# Gastroretentive Floating Microspheres of Metaxalone: A Novel Drug Delivery Approach for Muscle Relaxation

Brijesh Shukla [1], Akash Sharma [2*]

[1] Department of Pharmacy, Seiko College of Pharmacy, Harauni, Lucknow-226008, Uttar Pradesh, India

[2] Department of Pharmaceutical Sciences, School of Pharmaceutical Sciences, Babasaheb Bhimrao Ambedkar University, Lucknow-226025, Uttar Pradesh, India

## Article Info:

Article History:
Received 16 Aug 2025
Reviewed 27 Sep 2025
Accepted 23 Oct 2025
Published 15 Nov 2025

Cite this article as:

Shukla B, Sharma A, Gastroretentive Floating Microspheres of Metaxalone: A Novel Drug Delivery Approach for Muscle Relaxation, Journal of Drug Delivery and Therapeutics. 2025; 15(11):31-44 *DOI: http://dx.doi.org/10.22270/jddt.v15i11.7407*

*For Correspondence:

Mr. Akash Sharma, Research Scholar, Babasaheb Bhimrao Ambedkar University, Lucknow

## Abstract

Floating microspheres are advanced gastroretentive drug delivery systems that have the ability to extend gastric residence time and increase the oral bioavailability of drugs having narrow absorption windows. This research aimed to develop and characterize floating microspheres of metaxalone to address its short half-life and poor bioavailability, thereby enhancing its therapeutic action. Microspheres were prepared by ionotropic gelation with the aid of sodium alginate, ethylcellulose, HPMC, and sodium bicarbonate as a gas-forming agent. The systems were evaluated in a routine manner for micromeritic characteristics, entrapment efficiency, buoyancy, in vitro release patterns, and stability. Physicochemical interactions were studied by FTIR and DSC, whereas morphology was viewed through SEM. The optimized formulation (F5) had 58.43% entrapment efficiency, 81.32% buoyancy, and 82.34% sustained drug release within 12 h. SEM micrographs illustrated spherical particles with hollow cores, and compatibility studies established the lack of drug–polymer interaction. Stability studies showed minimal fluctuation in drug release and buoyancy during the storage time. Metaxalone-loaded floating microspheres had controlled release and extended gastric retention, indicating their usefulness to increase bioavailability, minimize dosing frequency, and enhance patient compliance in the therapy of muscle relaxation.

**Keywords**: Gastro-retentive drug delivery, floating microspheres, oral drug delivery systems, hollow microspheres, bioavailability enhancement.

## INTRODUCTION

Floating Drug Delivery Systems (FDDS) were first described by Davis in 1968 as an innovative strategy to prolong the residence time of dosage forms in the upper gastrointestinal tract (GIT). [1] These systems are designed to remain buoyant on gastric fluids due to their low density, allowing the drug to be released gradually over an extended period. [2] By maintaining prolonged gastric residence time (GRT), FDDS ensure sustained drug release, minimize plasma concentration fluctuations, and enhance therapeutic efficacy. [3] This approach is particularly beneficial for drugs with a narrow absorption window in the upper GIT, drugs unstable or poorly soluble in alkaline environments, and drugs with better solubility in acidic pH. [4]

FDDS are broadly classified into effervescent and non-effervescent systems. Effervescent systems contain gas-generating agents, such as sodium bicarbonate or citric acid, which release carbon dioxide upon contact with gastric fluid. The generated gas reduces the density of the dosage form, thereby promoting buoyancy. [5] Non-effervescent systems, including hydrodynamically balanced systems (HBS), employ gel-forming polymers such as hydroxypropyl methylcellulose (HPMC), polyacrylates, or sodium alginate. These polymers swell upon hydration, entrapping air within the matrix to maintain flotation. [6] Other strategies include raft-forming systems, where viscous gels entrap gas to create a floating barrier, and low-density or microballoon systems composed of hollow microspheres with intrinsic buoyancy. [7]

Microspheres, a key application of FDDS, are discrete spherical particles with a size range of 1-1000 µm. They may be biodegradable, synthetic, magnetic, radioactive, or bioadhesive. [8] Floating microspheres, generally prepared using polymers such as ethylcellulose, Eudragit, or chitosan, are preferred due to their large surface area, uniform drug distribution, and ability to sustain drug release while remaining buoyant. [9] The floating ability is attributed to air-filled cavities or hollow cores within the polymer matrix, produced via solvent evaporation, diffusion, or gas-forming methods. [10] Magnetic microspheres can be directed to targeted sites using external magnetic fields, whereas bioadhesive

microspheres improve gastric retention by adhering to the mucosal lining. [11]

The major advantages of FDDS include improved bioavailability of drugs absorbed in the upper GIT, reduced dosing frequency, better patient compliance, and applicability for both local and systemic delivery. However, patients with gastrointestinal motility disorders, rapid gastric emptying, or variable gastric pH conditions may experience limited effectiveness. [13] FDDS have been widely explored for delivering antibiotics (e.g., amoxicillin for Helicobacter pylori eradication), antacids, cardiovascular drugs, and anticancer agents. [14]

Preparation techniques for floating microspheres include single and double emulsion solvent evaporation for hydrophobic and hydrophilic drugs, respectively. [15] Other approaches involve coacervation phase separation for heat-sensitive drugs, spray drying for uniform particle size, solvent diffusion evaporation for hollow structures, and ionotropic gelation for polyelectrolyte-based systems. [16] The choice of method depends on drug solubility, polymer compatibility, and desired release profile. [17]

FDDS, particularly floating microspheres, offer a promising approach to enhance therapeutic efficacy for drugs exhibiting site-specific absorption in the stomach and upper intestine. [17] Their ability to combine controlled drug release with prolonged gastric retention underscores their relevance in modern pharmaceutical formulation. Recent research continues to optimize buoyancy, drug loading, and release kinetics to improve clinical utility. [18] Similar strategies have enhanced solubility and bioavailability for poorly soluble drugs like curcumin through non-aqueous self-emulsifying nanoemulsions[19], supporting the development of gastroretentive microspheres for metaxalone to improve therapeutic performance. [20]

### Aim and Objective

Oral administration continues to be the most convenient and widely preferred route for delivering drugs to conscious patients, despite the advancement of numerous modern dosage forms. Among the innovative approaches, floating drug delivery systems offer distinct advantages by prolonging gastric residence time and ensuring sustained drug release in the stomach. The present investigation focuses on improving the bioavailability of metaxalone, a centrally acting skeletal muscle relaxant, through the formulation and evaluation of floating microspheres designed for extended gastric retention. Metaxalone has a short elimination half-life of approximately 5–6 hours and a low oral bioavailability of about 25%, which necessitates multiple daily doses to sustain therapeutic plasma concentrations. Its rapid absorption from the stomach, coupled with quick systemic clearance, makes it a suitable candidate for a gastro-retentive floating system. In this formulation, ethyl cellulose serves as a low-density polymer to confer buoyancy, hydroxypropyl methylcellulose (HPMC) is incorporated to achieve controlled release, and sodium alginate is employed as a natural biopolymeric matrix for efficient drug entrapment. Sodium bicarbonate functions as the effervescent agent generating $CO_2$ to facilitate floating, while calcium chloride is utilized as a cross-linking agent. Clinically, metaxalone is indicated for relieving pain and discomfort in rheumatologic, orthopedic, and traumatic musculoskeletal conditions, usually in combination with analgesics and rest. Although its exact mechanism remains uncertain, it is postulated to act via central nervous system (CNS) depression rather than direct skeletal muscle effects. The drug is generally well tolerated, with mild CNS-related adverse reactions such as dizziness, drowsiness, headache, irritability, nausea, and vomiting.

## DRUGS, POLYMERS, AND METHODS

### Drugs and Chemicals

Metaxalone, a skeletal muscle relaxant, was obtained from Solitaire Pharmacia Pvt. Ltd., Chandigarh, India. Analytical-grade excipients were procured from various suppliers: sodium alginate from SD Fine Chem Ltd., sodium bicarbonate from SRIT Datia, ethanol from Merck, calcium chloride from Qualigens, hydroxyethyl cellulose (HEC) from Loba Chemie, glacial acetic acid from Fisher Scientific, and sodium carboxymethyl cellulose (NaCMC) from Himedia.

### Instruments and Apparatus:

### The following equipment was employed:

- 26G syringe needle, 10 cm long, from Hindustan Syringes and Medical Devices Ltd.
- Magnetic stirrer (Simco Microscope)
- UV–Visible Double Beam Spectrophotometer (2201 Systronics)
- Electronic balance (Contech)
- Whatman filter paper (Pall–Gelman Science)
- USP Standard dissolution apparatus (Veego)
- Melting point apparatus (Rolex)

### Methods

### Determination of Melting Point

The melting point of metaxalone was determined using the capillary method. The powdered drug was filled into a capillary tube, sealed at one end, and placed in the melting point apparatus. The temperature at which the first signs of melting appeared was recorded.

### UV Spectrophotometric Analysis

A stock solution (1 mg/mL) of Metaxalone was prepared using phosphate buffer (pH 7.4) and 0.1 N HCl (pH 1.2). Serial dilutions (5–30 µg/mL) were made from the stock. The absorbance was measured between 200 and 400 nm to determine λmax for each medium.

The spectrophotometric method used in this study was developed and validated in accordance with standard analytical quality-by-design (AQbD) principles to ensure precision and reproducibility, as previously demonstrated by Srujani et al. in related RP-HPLC and UV analytical method developments for Duvelisib, Pemigatinib, and Tenofovir determination (Srujani et al., 2020; Srujani et al., 2021b).

### Fourier Transform Infrared (FTIR) Spectroscopy

FTIR spectra were recorded using the KBr pellet method in the range of 400–600 $cm^{-1}$. The drug was mixed with potassium bromide and compressed into pellets using a hydraulic press. The spectra of the sample were compared with those of pure metaxalone for confirmation.

### Solubility Studies

One milligram of metaxalone was dissolved in 1 mL of various solvents and buffer systems to assess solubility characteristics.

### Calibration Curve Preparation

A standard solution of metaxalone (10 mg in 100 mL) was prepared separately in phosphate buffer (pH 7.4) and 0.1 N HCl. Serial dilutions were made, and absorbance was measured at λmax: 259 nm (water), 375 nm (phosphate buffer pH 7.4), and 265 nm (0.1 N HCl).

### Polymer Identification

The chemical compatibility of sodium alginate with metaxalone was checked using FTIR spectroscopy in the 400-600 $cm^{-1}$ range.

### Drug Excipient Compatibility Studies

The drug and each excipient were blended in a 1:1 ratio and stored in glass vials under accelerated stability conditions (25°C/75% RH and 60°C/75% RH) for two months. Both open and sealed vials were used. Physical changes were noted at weekly intervals. FTIR analysis was conducted to detect any chemical interactions.

### Formulation Table

**Table 1: Metaxalone alginate microspheres were prepared via ionotropic gelation using varying polymer ratios.**

| Formulation Code | Metaxalone (mg) | NaCMC (mg) | HEC (mg) | $NaHCO_3$ (mg) | Na-Alg (mg) | $CaCl_2$ (%) |
|---|---|---|---|---|---|---|
| F1 | 500 | 0.75 | 0.5 | 250 | 1.5 | 4 |
| F2 | 500 | 0.75 | 100 | 250 | 1.5 | 4 |
| F3 | 500 | 100 | 0.75 | 50 | 1.5 | 4 |
| F4 | 500 | 150 | 0.5 | 125 | 1.5 | 4 |
| F5 | 500 | 100 | 1.5 | 50 | 1.5 | 4 |
| F6 | 500 | 225 | 0.75 | 100 | 1.5 | 4 |
| F7 | 500 | 0.75 | 0.5 | 250 | 1.5 | 4 |
| F8 | 500 | 0.75 | 0.5 | 250 | 1.5 | 4 |
| F9 | 500 | 0.75 | 100 | 250 | 1.5 | 4 |
| F10 | 500 | 100 | 0.75 | 50 | 1.5 | 4 |

### Evaluation of Prepared Microspheres

### Micromeritic Properties

Bulk density, tapped density, angle of repose, Hausner's ratio, and Carr's compressibility index were measured to determine flow properties.

### Particle Size Distribution

Microspheres (1 g) were passed through a series of sieves of different mesh sizes. The fraction retained on each sieve was weighed, and the mean particle size was calculated.

### Density Measurements

Loose bulk density (LBD) and tapped bulk density (TBD) were calculated using a graduated cylinder. To determine the tapped bulk density (TBD), the graduated cylinder was tapped 100 times.

### Formulas:

LBD = Mass of microspheres / Volume before tapping

TBD = Mass of microspheres / Volume after tapping

### Angle of Repose

The funnel method was used to determine the angle of repose (θ):

$\theta = \tan^{-1}(h / r)$

### Carr's Index and Hausner's Ratio

Carr's Index = [(TBD – LBD) / TBD] × 100

Hausner's Ratio = TBD / LBD

### Percentage Yield

% Yield = (Practical weight / Theoretical weight) × 100

### Drug Entrapment Efficiency

The percentage of entrapment is calculated as (Actual drug content / Theoretical drug content) × 100.

### Buoyancy Test

Microspheres (500 mg) were dispersed in simulated gastric fluid (pH 1.2) containing 0.02% Tween 20 and

stirred at 100 rpm for 4 h. Floating and settled fractions were separated, dried, and weighed.

% Buoyancy = [Wf / (Wf + Ws)] × 100

Differential Scanning Calorimetry (DSC)

Samples (2 mg) were heated from 25°C to 200°C under nitrogen flow (30 mL/min) to assess thermal behavior.

### In Vitro Drug Release

Dissolution testing was conducted using USP basket apparatus at 50 rpm in 900 mL of medium maintained at 37 ± 1°C. Samples (5 mL) were withdrawn at predetermined intervals, filtered (0.25 µm), and analyzed spectrophotometrically.

### Stability Studies

Optimized microsphere formulations were stored in sealed glass vials at 25 ± 5°C / 75% RH and 40 ± 5°C / 75% RH for three months. Poststorage, buoyancy and drug release profiles were re-evaluated to assess stability.

## RESULTS AND DISCUSSION

### Identification Test for Drugs

*Melting Point Determination*

Metaxalone's melting point was 122°C, indicating purity, according to the literature and pharmacological profile. The Digital Melting Point Apparatus measured the drug's melting point.

*Solubility*

**Table 2: Solubility of Metaxalone**

| S.No. | Solvents | Result |
|---|---|---|
| **1** | Water | Freely Soluble |
| **2** | Alcohol | Partially Soluble: after half an hour, residue remained in the test tube. |
| **3** | Ether | Not Soluble |
| **4** | Acetone | Not Soluble |

*UV-Spectrophotometry*

Research using ultraviolet spectroscopy was conducted in three distinct mediums ranging from 220 nm to 440 nm: water, where the highest value observed was 259.2 nm in water, while the highest value in the other medium was 375 nm.

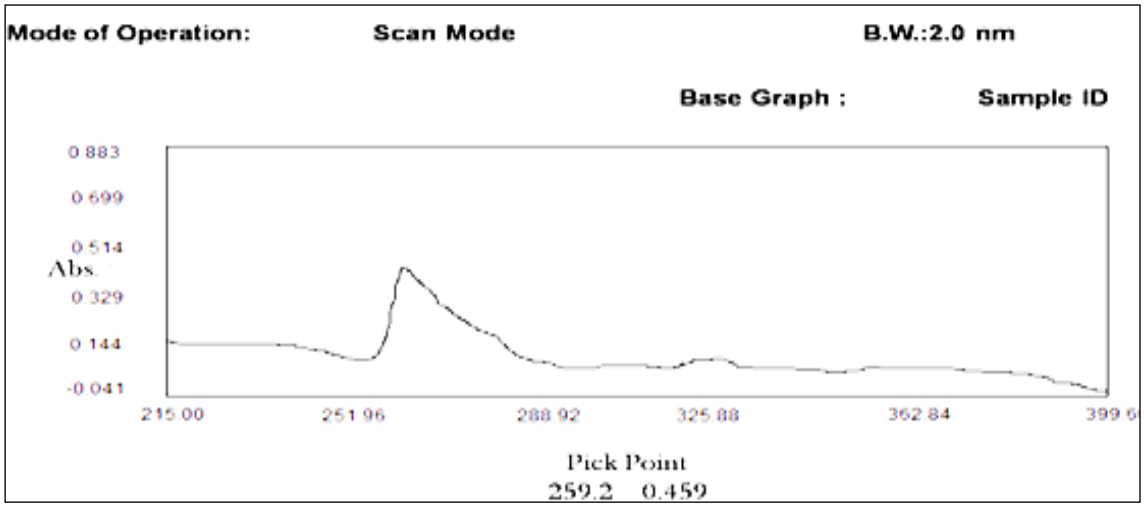


**Figure 1: λmax Scan for Metaxalone at 259.2 nm in Water**

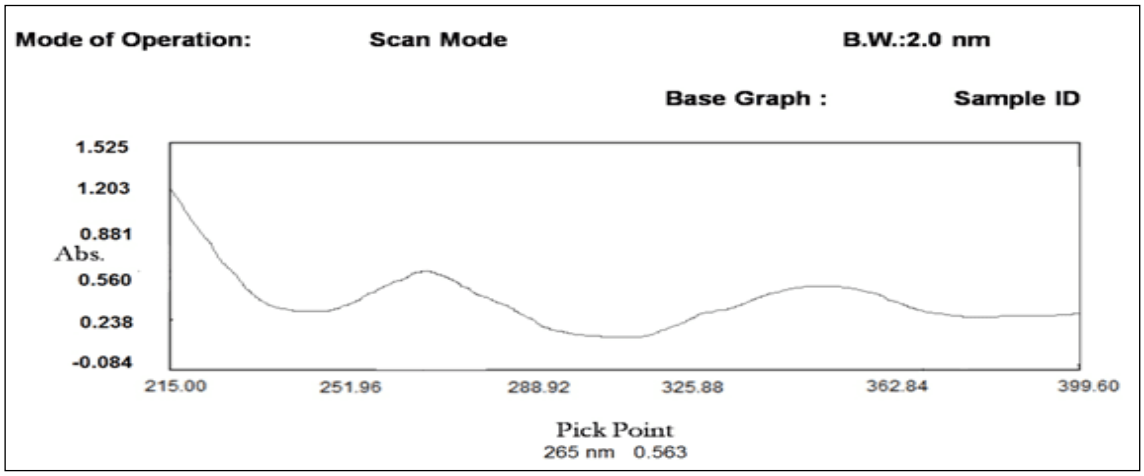


**Figure 2: λmax Scan for Metaxalone at 265 nm in 0.1 N HCl pH 1.2**

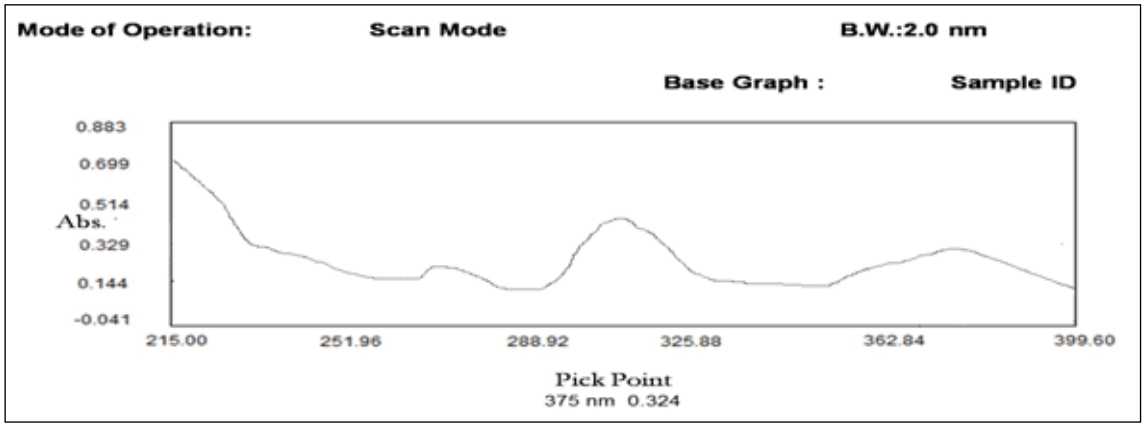


**Figure 3: λmax Scan for Metaxalone at 375 nm in Phosphate Buffer pH 7.4**

**FTIR Spectra of Pure Drug**

Below the figure is a comparison of the FTIR spectra obtained from a pure metaxalone sample and a standard functional group.

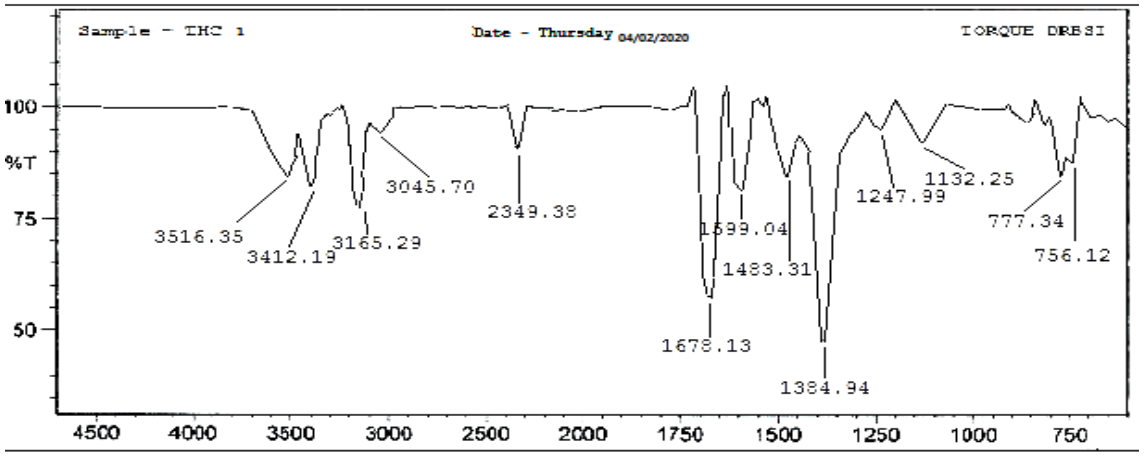


**Figure 4 FTIR Spectra of Metaxalone**

**Table 3: IR Frequencies for Metaxalone**

| Functional Group | Observed frequencies ($cm^{-1}$) |
|---|---|
| **NH Stretching** | 3516.35 |
| **OH Stretching** | 3045.7 |
| **C=O Stretching** | 1678.13 |
| **C=C Stretching** | 1599.04 |

The process involves the preparation of a calibration curve for the purpose of estimating the drug concentration.

The drug is diluted in different solvents at a concentration of 10 g/ml, and when using the spectrophotometer for the λmax run, the maximum wavelength is found to be 259 nm with an absorbance of 0.459.

Calibration curve in water

**Table 4: Calibration Curve Readings**

| S.No. | Concentration (µg/ml) | λ µαξ (νµ) | Absorbance |
|---|---|---|---|
| 1 | 2 | 259 | 0.072 |
| 2 | 4 | 259 | 0.165 |
| 3 | 6 | 259 | 0.252 |
| 4 | 8 | 259 | 0.338 |
| 5 | 10 | 259 | 0.459 |

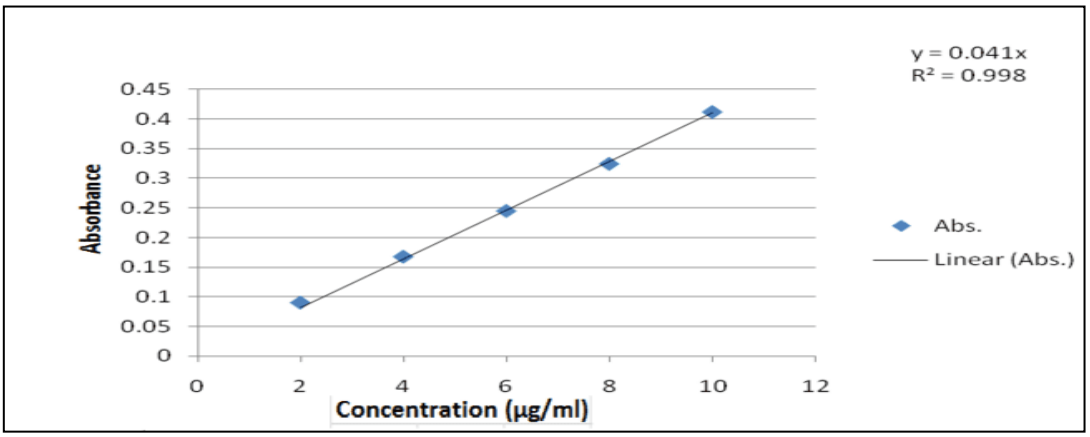


**Figure 5: Calibration Curve of Metaxalone in Water**

*Calibration curve in buffer 7.4*

**Table 5: Calibration Curve Readings**

| S.No. | Concentration (µg/ml) | λ µαξ (νµ) | Absorbance |
|---|---|---|---|
| 1 | 2 | 375 | 0.091 |
| 2 | 4 | 375 | 0.168 |
| 3 | 6 | 375 | 0.245 |
| 4 | 8 | 375 | 0.324 |
| 5 | 10 | 375 | 0.411 |

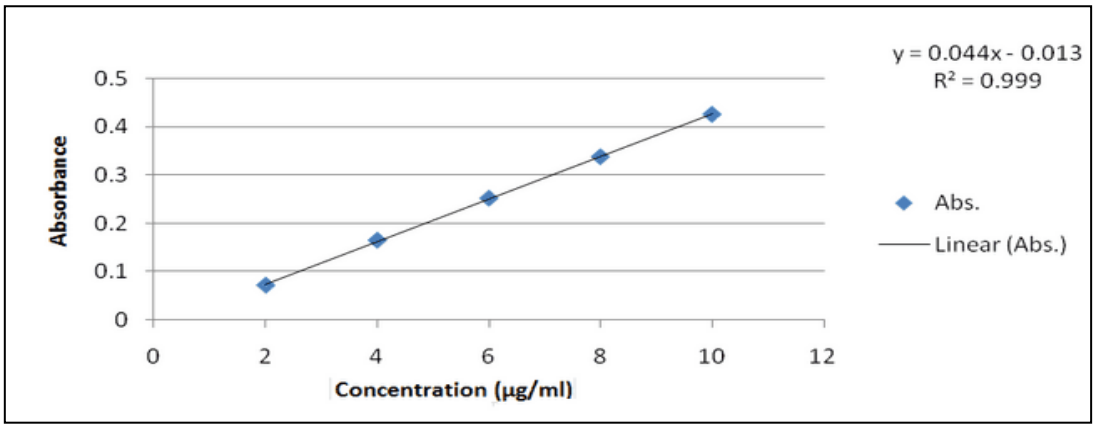


**Figure 6: Calibration Curve of Metaxalone in Buffer 7.4**

*Calibration curve in 0.1 N HCl*

**Table 6: Calibration Curve Readings**

| S.No. | Concentration (µg/ml) | λ µαξ (νµ) | Absorbance |
|---|---|---|---|
| 1 | 2 | 265 | 0.104 |
| 2 | 4 | 265 | 0.178 |
| 3 | 6 | 265 | 0.275 |
| 4 | 8 | 265 | 0.419 |
| 5 | 10 | 265 | 0.511 |

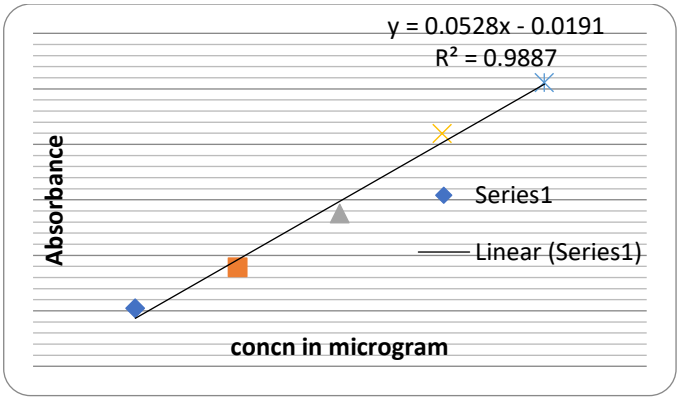


**Figure 7: Calibration Curve of Metaxalone in 0.1 N HCl**

**Table 7: Loss on drying reading**

| S.No. | Time interval | Wt. of Drug | Wt. of Petri dish | Total Wt. |
|---|---|---|---|---|
| 1 | 0 min | 500 mg | 48.310 gm | 48.81 gm |
| 2 | 30 min | 480 mg | 48.310 gm | 48.79 gm |
| 3 | 60 min | 475 mg | 48.310 gm | 58.78 gm |
| 4 | 90 min | 470 mg | 48.310 gm | 48.71 gm |
| 5 | 150 min | 470 mg | 48.310 gm | 48.71 m |

**Loss on drying**

The loss on the drying method involves weighing a 500 mg medication dosage into a Petri dish and heating it in a hot air oven at 105°C until weight loss ceases after a predetermined time.

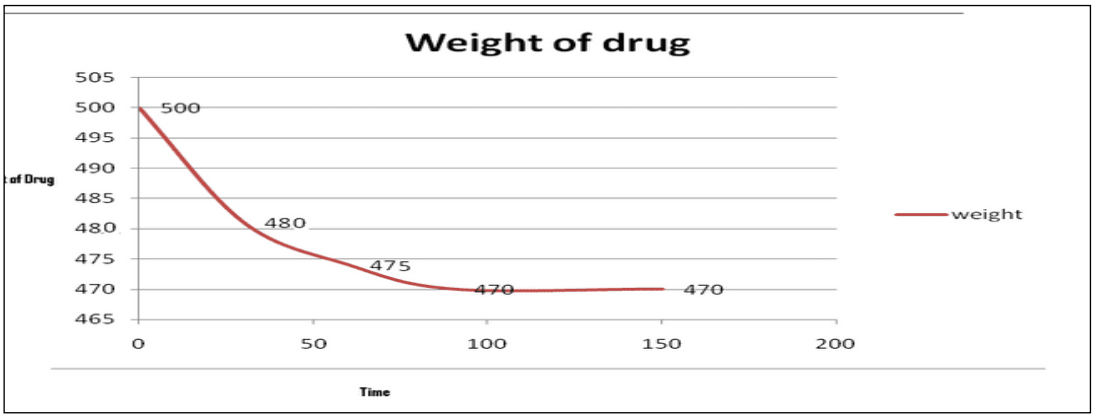


**Figure 8: Loss on Drying Curve of Metaxalone**

**Identification of polymer used**

The obtained sample was determined to be pure ethyl cellulose and sodium alginate because the FTIR spectrometer recorded their IR spectra, as shown in the figure, and compared them to the standard functional group frequencies of the two substances. The results showed that both ethyl cellulose and sodium alginate fell within the reported range of frequencies.

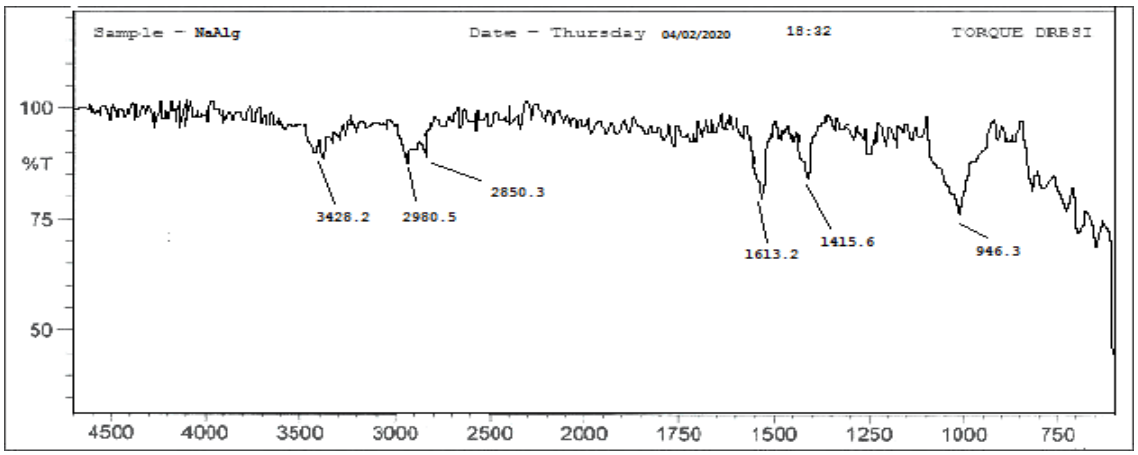


**Figure 9: FT-IR spectra of sodium alginate**

**Table 8: FT-IR frequencies of Sodium Alginate**

| S.No. | Functional Group | Observed Frequencies ($cm^{-1}$) |
|---|---|---|
| 1 | Oh, stretching. | 3428 |
| 2 | CH stretching | 2980 |
| 3 | $-CH_2$ | 1613 |

**Compatibility studies between drug and excipient**

The drug-excipient compatibility tests involved taking samples that had been stored under different accelerated circumstances and analyzing their physical properties, such as how their color changed at different intervals.

Infrared spectroscopy was used to conduct the investigation of the drug-polymer interaction. We used an FTIR spectrophotometer (PERKIN ELIMER BX) to acquire the infrared spectra of the drug and different polymers that would be employed in the formulation. We then compared these spectra to the individual spectra.

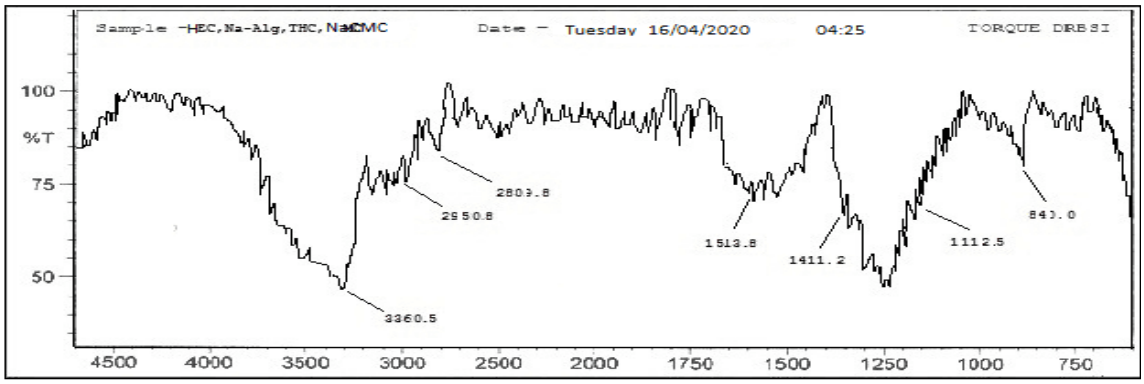


**Figure 10: FTIR of Drug and Excipient**

**Table 9: IR Frequencies of Drug and Excipient**

| S.No. | Functional Groups | Observed frequencies ($cm^{-1}$) |
|---|---|---|
| 1 | NH- stretching | 3360.5 |
| 2 | OH-stretching | 2950.8 |
| 3 | CH-stretching | 2809.8 |
| 4 | C=O stretching | 1513.8 |
| 5 | $-COO^-$ stretching vibration | 1411.2 |
| 6 | C-C stretch | 1112.5 |
| 7 | C-H roking | 840 |

**Table 10: Physical Compatibility Studies**

| Temperature and humidity | | 0 Days | 15 Days | 30 Days | 60 Days |
|---|---|---|---|---|---|
| **25°C ±2°C/75% RH ± 5%** | **A1** | No change | No change | No change | No change |
| | **B1** | No change | No change | No change | No change |
| | **C1** | No change | No change | No change | No change |
| **60°C ±2°C/75% RH ± 5%** | **A2** | No change | No change | No change | No change |
| | **B2** | No change | No change | No change | No change |
| | **C2** | No change | No change | No change | No change |

Take a sample that has been in storage for at least 60 days and run it through an FTIR analyzer to find out whether the chemicals are compatible. Based on the data in the table, it seems that both the pure drug and combination spectra have comparable peaks; hence, drug-polymer interaction is not present.

The Metaxalone FTIR spectrum was obtained using the Potassium Bromide Disc Method with a Fourier transform infrared spectrophotometer (PERKIN ELMER BX). The identification and purity of the medicine were validated upon comparison of the discovered major peaks with the reference FTIR spectra of Metaxalone. Neither the pure drug nor the combination spectra demonstrate drug-polymer interaction due to identical peaks.

**Evaluation of Prepared Microspheres**

**Micromeritics characterization**

**Table 11: Micromeritics study of formulated microspheres**

| Formulation Code | Angle of Repose ± SD | Tapped SD | Bulk Density ± SD | Carr's Index ± SD | Hausner's Ratio ± SD |
|---|---|---|---|---|---|
| **F1** | 21.241±0.010 | 0.641±0.012 | 0.410±0.022 | 9.345±0.120 | 1.031±0.024 |
| **F2** | 22.431±0.031 | 0.662±0.004 | 0.482±0.002 | 10.121±0.216 | 1.118±0.014 |
| **F3** | 25.840±0.012 | 0.542±0.010 | 0.498±0.008 | 11.328±1.421 | 1.106±0.032 |
| **F4** | 24.620±0.110 | 0.492±0.011 | 0.532±0.018 | 11.524±1.598 | 1.132±0.034 |
| **F5** | 22.324±0.012 | 0.521±0.060 | 0.598±0.163 | 10.369±0.436 | 1.210±0.124 |
| **F6** | 26.012±0.019 | 0.612±0.010 | 0.564±0.019 | 11.324±1.457 | 1.160±0.063 |
| **F7** | 23.160±0.022 | 0.542±0.022 | 0.498±0.026 | 11.587±0.254 | 1.131±0.120 |
| **F8** | 27.113±0.115 | 0.513±0.024 | 0.641±0.036 | 12.342±0.254 | 1.140±0.082 |
| **F9** | 19.118±0.014 | 0.523±0.018 | 0.602±0.021 | 7.185±0.651 | 1.006±0.026 |
| **F10** | 22.124±0.016 | 0.512±0.014 | 0.501±0.012 | 7.233±1.341 | 1.032±0.061 |

**Table 12: Drug entrapment efficiency, percent yield, % buoyancy, and drug content of microspheres.**

| Formulation Code | % Drug entrapment efficiency | % Yield | % Buoyancy | Theoretical drug content (gm) | Actual drug content (gm) |
|---|---|---|---|---|---|
| **F1** | 68.48 | 61.45 | 68.4 | 0.5 | 0.3642 |
| **F2** | 60.34 | 60.32 | 68.6 | 0.5 | 0.362 |
| **F3** | 68.34 | 63.21 | 76.3 | 0.5 | 0.3562 |
| **F4** | 57.34 | 58.32 | 70.25 | 0.5 | 0.3642 |
| **F5** | 58.43 | 61.32 | 81.32 | 0.5 | 0.3732 |
| **F6** | 59.38 | 58.36 | 70.25 | 0.5 | 0.3754 |
| **F7** | 66.38 | 62.38 | 70.32 | 0.5 | 0.3553 |
| **F8** | 69.29 | 70.34 | 72.65 | 0.5 | 0.3653 |
| **F9** | 67.95 | 66.32 | 74.21 | 0.5 | 0.3685 |
| **F10** | 60.35 | 59.34 | 78.12 | 0.5 | 0.3102 |

**Morphological characteristics of the microspheres:**

The ionotropic gelation process produced floating microspheres of metaxalone that were characterized by being of the monolithic matrix type, discrete, spherical, and free-flowing. Consistently, the microcapsules' sizes varied from 300 µm. Microcapsules were found to be completely spherical and covered by the coat polymer in their scanning electron microscope photos.

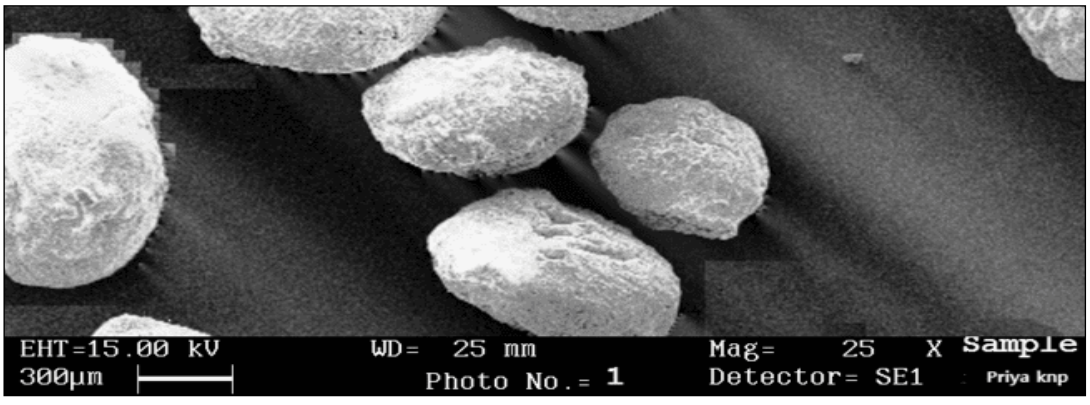


**Figure 11: Small spheres, measuring around 300 to 900 µm in diameter.**

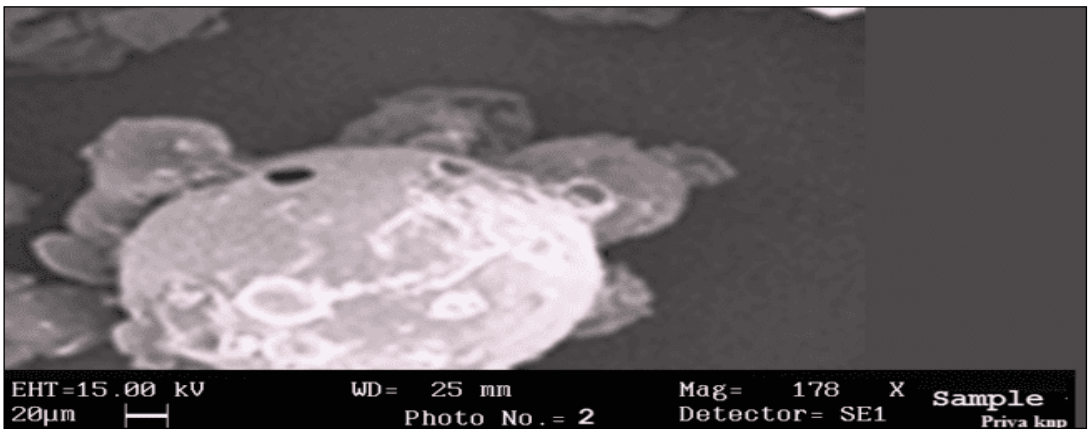


**Figure 12: Size of an Individual Microsphere**

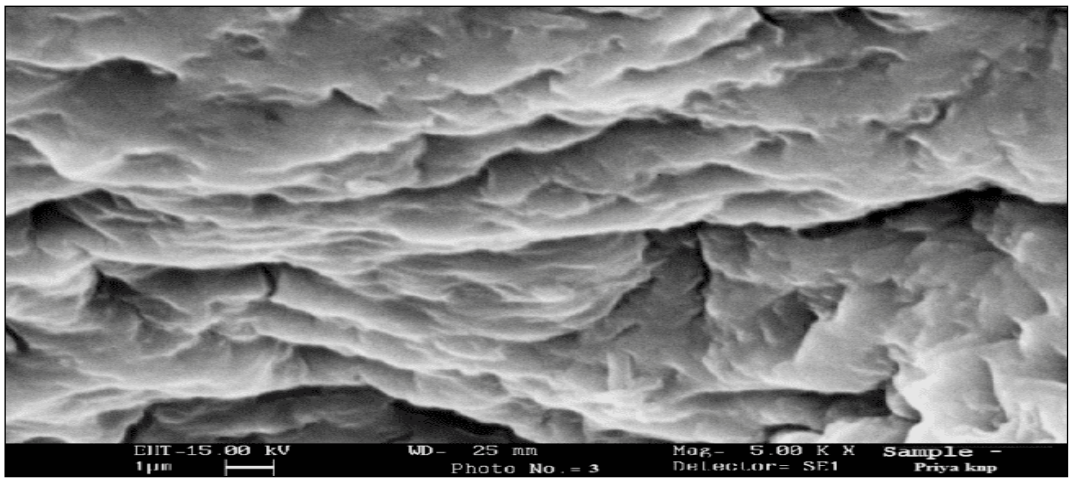


**Figure 13: Texture of individual microspheres**

### Differential Scanning Calorimetry (DSC)

For checking the melting point of the pure metaxalone drug, DSC is taken and is observed near about 194°C.

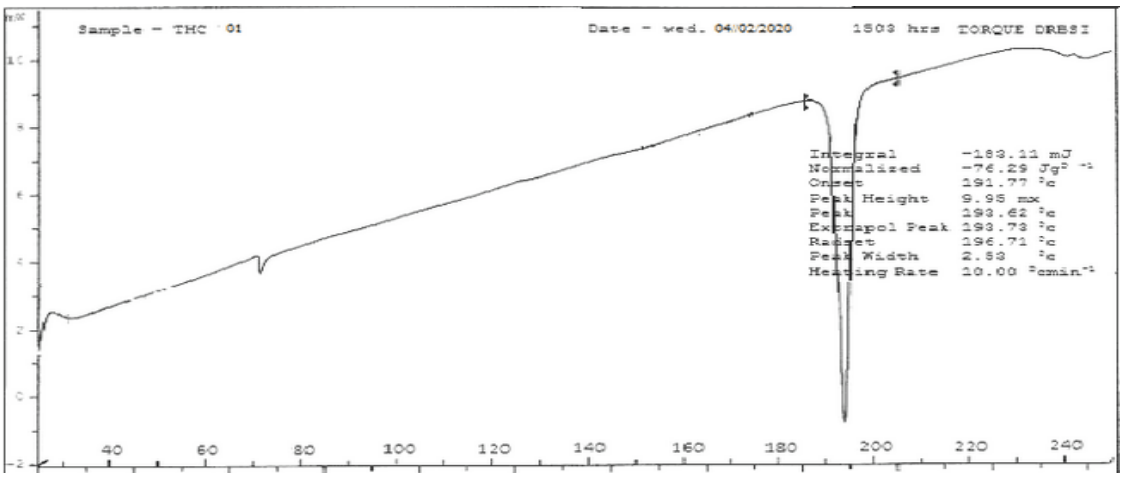


**Figure 14: Pure medication differential scanning calorimetry**

There was a single endothermic peak at 194°C on the DSC curve of Metaxalone. At around 165°C, the improved formulation shows a low-intensity peak in the DSC profile. That the formulation's crystallinity is decreased and that the drug and polymer do not interact is shown conclusively by this.

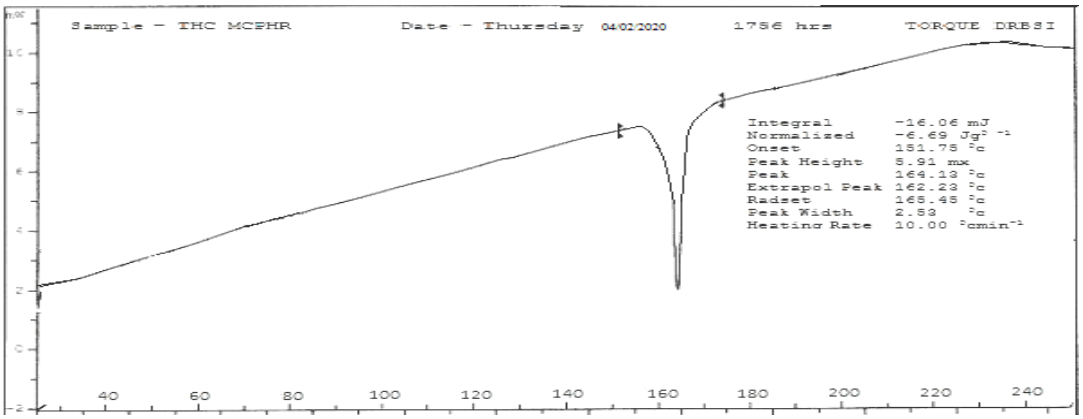


**Figure 15: An Analysis of Thiocolchicoside Microspheres by Differential Scanning Calorimetry (DSC)**

### In vitro dissolution studies

In vitro drug release testing was performed on the prepared microspheres in 900 mL of hydrobromic acid (HBr) buffer at a pH of 1.2. An eight-stage basket-type dissolving rate equipment (Veego) that is typical for the USP was used to perform the investigation. All through the experiment, the dissolving media was kept at a steady 37 ± 0.5°C while the baskets were spun at a rate of 50 revolutions per minute (rpm) to mimic circumstances in the gastrointestinal tract.

### Accelerated Stability Studies

One way to gauge the quality of dosage forms is by looking at their stability in preparation. As a result, the stability of microspheres loaded with metaxalone was the subject of expedited testing. When compared to the microspheres loaded with metaxalone before storage in the stability chamber, physical characteristics, including color, surface shape, and particle movement, showed little change, according to the data. The floating ratio and medication loading also changed very little.

**Table 13: Profile of in vitro release of microspheres containing metaxalone**

| Time | F1 | F2 | F3 | F4 | F5 | F6 | F7 | F8 | F9 | F10 |
|---|---|---|---|---|---|---|---|---|---|---|
| (hr) | % Drug Release F1 | % Drug Release F2 | % Drug Release F3 | % Drug Release F4 | % Drug Release F5 | % Drug Release F6 | % Drug Release F7 | % Drug Release F8 | % Drug Release F9 | % Drug Release F10 |
| 0 | 0 | 0 | 0 | 0 | 0 | 0 | 0 | 0 | 0 | 0 |
| 1.5 | 18.24 | 17.21 | 26.21 | 20.2 | 23.91 | 17.23 | 22.12 | 25.31 | 18.35 | 17.21 |
| 3 | 24.32 | 25.31 | 30.29 | 29.41 | 31.32 | 25.31 | 30.12 | 32.31 | 27.42 | 27.35 |
| 4.5 | 35.32 | 38.22 | 39.32 | 37.31 | 39.65 | 34.45 | 39.34 | 39.34 | 36.62 | 35.25 |
| 6 | 43.39 | 49.35 | 49.24 | 45.37 | 50.42 | 41.32 | 52.15 | 47.56 | 47.52 | 45.96 |
| 7.5 | 51.27 | 54.85 | 60.21 | 57.48 | 54.95 | 48.35 | 60.32 | 56.25 | 52.52 | 52.45 |
| 9 | 68.24 | 66.65 | 65.31 | 62.35 | 65.45 | 58.52 | 64.45 | 64.87 | 60.24 | 60.42 |
| 11 | 72.34 | 70.21 | 71.1 | 70.14 | 73.34 | 67.32 | 68.14 | 73.21 | 67.81 | 67.45 |
| 12 | 78.37 | 76.02 | 80.32 | 80.21 | 82.34 | 75.98 | 77.85 | 80.32 | 77.41 | 77.68 |

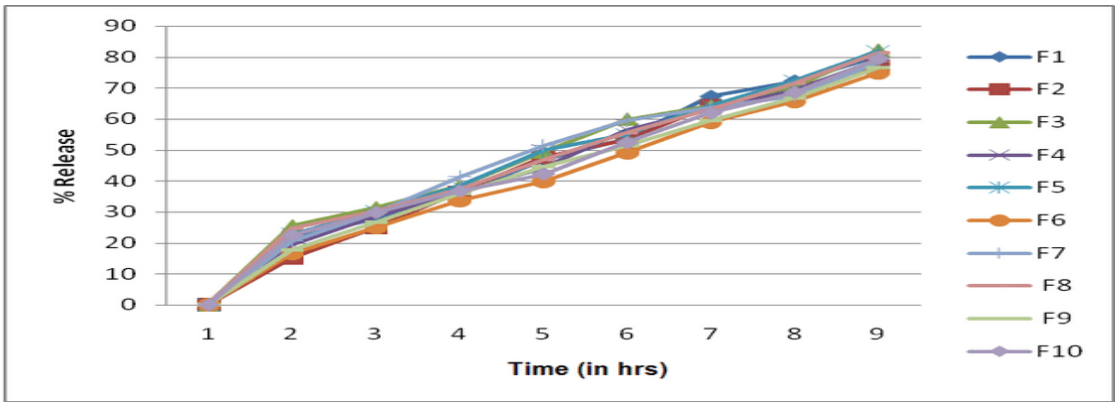


**Figure 16: Shows the drug release percentage of the optimized formulation, which is 16 %**

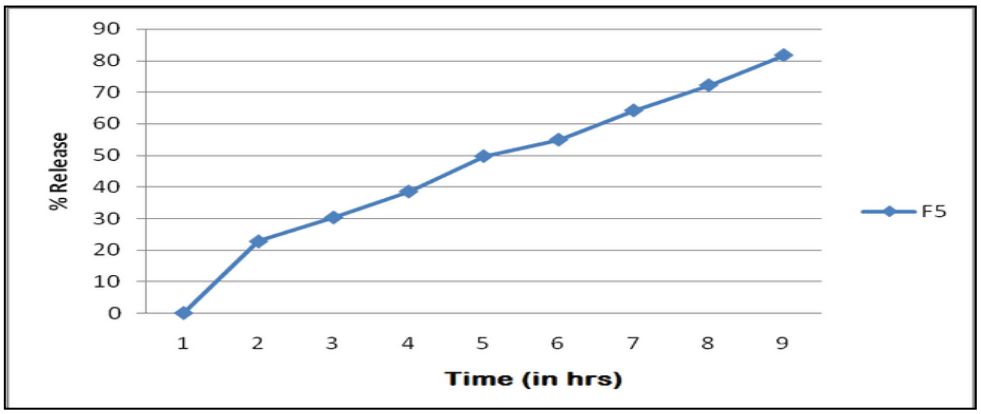


**Figure 17: Drug release versus time graphs for each formulation**

**Table 14: Accelerated optimized formulation stability study**

| Temperature & percentage relative humidity | Items | | Days | | | |
|---|---|---|---|---|---|---|
| | | | 0 | 30 | 60 | Color |
| 25±5°C & 75% RH | % Buoyancy | F5 | 74.6 | 70.4 | 64.20 | Brownish yellow in color |
| | %Drug release | F5 | 82.4 | 80.4 | 80.09 | Brownish yellow in color |
| 40±5°C & 75% RH | % Buoyancy | F5 | 72.4 | 71.3 | 67.43 | Brownish yellow in color |
| | %Drug release | F5 | 81.2 | 81.3 | 80.54 | Brownish yellow in color |

## DISCUSSION

This study aimed to manufacture gastroretentive floating microspheres of metaxalone to address its restricted oral bioavailability and brief half-life. The formulated products exhibited satisfactory micromeritic properties, indicating favorable flow characteristics and suitability for large-scale production. Entrapment effectiveness varied from 57% to 69%, with the optimal formulation (F5) achieving 58.43%. The entrapment effectiveness of alginate-based floating microspheres typically ranges from 50% to 70%, contingent upon the polymer ratio and drug solubility, as corroborated by previous studies (Pawar et al., 2011; Virmani and Gupta, 2017). Buoyancy is a crucial factor for stomach retention. The optimized microspheres in this study exhibited over 80% buoyancy for 12 hours, consistent with previous research employing sodium bicarbonate and ethylcellulose as gas-generating and low-density agents, respectively (Singh and Kim, 2000; Shah et al., 2009). The hollow internal structure identified using SEM further corroborated the buoyancy process. In vitro release studies indicated a sustained release of 82.34% over 12 hours for the improved batch. The delayed release profile can be ascribed to the synergistic use of sodium alginate and HPMC, which create a gel matrix that modulates drug transport, while ethylcellulose contributes hydrophobicity to further hinder release. Comparable biphasic release patterns have been seen for several muscle relaxants and centrally acting pharmaceuticals encapsulated in gastroretentive microspheres (Deshpande et al., 1996; Vrettos et al., 2021). DSC and FTIR analyses indicated a lack of significant drug–polymer interactions, while stability tests showed little change in buoyancy and release kinetics under accelerated conditions, affirming the formulation's robustness. The findings suggest that ionotropic gelation is an effective method for encapsulating metaxalone, preserving structural integrity, and ensuring predictable release performance. The produced floating microspheres exhibited prolonged gastric retention, sustained drug release, and enhanced entrapment efficiency. These qualities aim to enhance the bioavailability of metaxalone, decrease dosing frequency, and ultimately increase patient adherence. The findings align with previous research indicating that floating microspheres may serve as a viable approach for drugs characterized by a limited absorption window or brief half-life (Kotreka & Adeyeye, 2011; Ishak, 2015) The absence of significant drug–polymer interaction in the present work is consistent with our earlier findings on sulfamethoxazole derivatives, where compatibility and stability played a pivotal role in ensuring reproducible drug delivery outcomes (Sharma et al., 2025)."

The analytical estimation of metaxalone using spectrophotometric techniques followed a systematic validation approach, comparable to earlier AQbD-guided analytical methods established by Srujani et al. for various active pharmaceutical ingredients (Duvelisib, Fedratinib, and Pemigatinib). These studies highlight the importance of design of experiments (DoE)-based

optimization in achieving reproducible analytical precision and method robustness.

## CONCLUSION

The findings of this study indicate that the floating microsphere drug delivery system significantly enhances the gastrointestinal bioavailability of metaxalone. The formulation maintained buoyancy in gastric fluid, allowing the drug to dissolve gradually in the acidic environment and enter the systemic circulation in a controlled manner. This sustained release profile prolonged gastric residence time, resulting in more stable plasma drug concentrations compared to conventional oral dosage forms. Consequently, the approach offers the potential for reduced dosing frequency, improved therapeutic efficacy, and better patient compliance.

### List of Symbols and Abbreviations

| Abbreviation | Full Form |
|---|---|
| API | Active Pharmaceutical Ingredient |
| DMSO | Dimethyl Sulfoxide |
| FTIR | Fourier Transform Infrared Spectroscopy |
| GC | Gas Chromatography |
| HPLC | High-Performance Liquid Chromatography |
| IR | Infrared Spectroscopy |
| LC-MS | Liquid Chromatography–Mass Spectrometry |
| LOD | Limit of Detection |
| LOQ | Limit of Quantification |
| MS | Mass Spectrometry |
| NMR | Nuclear Magnetic Resonance |
| pKa | Acid Dissociation Constant |
| RP-HPLC | Reverse Phase High-Performance Liquid Chromatography |
| SEM | Scanning Electron Microscopy |
| TLC | Thin Layer Chromatography |
| UV | Ultraviolet |
| UV-Vis | Ultraviolet–Visible Spectroscopy |
| XRD | X-ray Diffraction |

**Acknowledgements:** The authors gratefully acknowledge the support of their respective institutions and research laboratories for providing the necessary facilities and infrastructure to carry out this work.

**Author Contributions:** Conceptualization: Brijesh Shukla; Methodology: Brijesh Shukla, Akash Sharma; Investigation: Brijesh Shukla; Writing Original Draft: Brijesh Shukla, Akash Sharma Writing Review & Editing: Brijesh Shukla, Akash Sharma; Supervision: Akash Sharma*.

**Funding Source:** This research did not receive any specific grant from funding agencies in the public, commercial, or not-for-profit sectors.

**Conflicts of Interest:** The authors declare that there are no conflicts of interest regarding the publication of this manuscript.

**Ethical Approval:** Not applicable. This study does not involve any human or animal testing.

## REFERENCES

1. Pawar VK, Kansal S, Garg G, Awasthi R, Singodia D, Kulkarni GT. Gastroretentive dosage forms: A review with special emphasis on floating drug delivery systems. Drug Deliv. 2011;18(2):97-110. https://doi.org/10.3109/10717544.2010.520354 PMid:20958237

2. Singh BN, Kim KH. Floating drug delivery systems: An approach to oral controlled drug delivery via gastric retention. J Control Release. 2000;63(3):235-59. https://doi.org/10.1016/S0168-3659(99)00204-7 PMid:10601721

3. Deshpande A, Shah N, Rhodes CT, Malick W. Controlled-release systems for delivering drugs that remain in the stomach for a prolonged period: An overview. Drug Dev Ind Pharm. 1996;22(6):531-39. https://doi.org/10.3109/03639049609108355

4. Avdeef A. Absorption and drug development: solubility, permeability, and charge state. 2nd ed. Hoboken (NJ): John Wiley & Sons; 2012. https://doi.org/10.1002/9781118286067

5. Kotreka UK, Adeyeye MC. Gastroretentive floating drug-delivery systems: A critical review. Crit Rev Ther Drug Carrier Syst. 2011;28(1):47-99. https://doi.org/10.1615/CritRevTherDrugCarrierSyst.v28.i1.20 PMid:21395515

6. Ishak RA. Buoyancy-generating agents for stomach-specific drug delivery: An overview with special emphasis on floating behavior. J Pharm Pharm Sci. 2015;18(1):77-100. https://doi.org/10.18433/J3602K PMid:25877444

7. Shah SH, Patel JK, Patel NV. Stomach-specific floating drug delivery system: A review. Int J PharmTech Res. 2009;1(3):623-33.

8. Virmani T, Gupta J. Pharmaceutical application of microspheres: An approach for the treatment of various diseases. Int J Pharm Sci Res. 2017;8(8):3253-60.

9. Thakral S, Thakral NK, Majumdar DK. Eudragit®: A technology evaluation. Expert Opin Drug Deliv. 2013;10(1):131-49. https://doi.org/10.1517/17425247.2013.736962 PMid:23102011

10. Vrettos NN, Roberts CJ, Zhu Z. Gastroretentive technologies in tandem with controlled-release strategies: A potent answer to oral drug bioavailability and patient compliance implications. Pharmaceutics. 2021;13(10):1591. https://doi.org/10.3390/pharmaceutics13101591 PMid:34683884 PMCid:PMC8539558

11. Hou JY, Li Y, Zhao N, Ji W, Ding Y, Zhang L, et al. Mucoadhesive microparticles for gastroretentive delivery: Preparation, biodistribution, and targeting evaluation. Mar Drugs. 2014;12(12):5764-87. https://doi.org/10.3390/md12125764 PMid:25470180 PMCid:PMC4278200

12. Garg R, Gupta GD. Progress in controlled gastroretentive delivery systems. Trop J Pharm Res. 2008;7(3):1055-66. https://doi.org/10.4314/tjpr.v7i3.14691

13. Keller J, Bassotti G, Clarke J, Dinning PG, Fox M, Grover M, et al. Advances in the diagnosis and classification of gastric and intestinal motility disorders. Nat Rev Gastroenterol Hepatol. 2018;15(5):291-308. https://doi.org/10.1038/nrgastro.2018.7 PMid:29622808 PMCid:PMC6646879

14. Roszczenko-Jasińska P, Wojtyś MI, Jagusztyn-Krynicka EK. Helicobacter pylori treatment in the post-antibiotics era is researching for new drug targets. Appl Microbiol Biotechnol. 2020;104(23):9891-905. https://doi.org/10.1007/s00253-020-10945-w PMid:33052519 PMCid:PMC7666284

15. O'Donnell PB, McGinity JW. Preparation of microspheres by the solvent evaporation technique. Adv Drug Deliv Rev. 1997;28(1):25-42. https://doi.org/10.1016/S0169-409X(97)00049-5 PMid:10837563

16. Gouin S. Microencapsulation: Industrial appraisal of existing technologies and trends. Trends Food Sci Technol. 2004;15(7-8):330-47. https://doi.org/10.1016/j.tifs.2003.10.005

17. Kamaly N, Yameen B, Wu J, Farokhzad OC. Degradable controlled-release polymers and polymeric nanoparticles: Mechanisms of controlling drug release. Chem Rev. 2016; 2016;116(4):2602-63. https://doi.org/10.1021/acs.chemrev.5b00346 PMid:26854975 PMCid:PMC5509216

18. Tayal S, Sharma A, Kumar A. Development and characterization of non-aqueous-based self-emulsifying nanoemulsion of curcumin. Middle East J Appl Sci Technol. 2023;6(2):144-52. https://doi.org/10.46431/MEJAST.2023.6216

19. Haseen M, Katiyar PK, Shukla B, Sharma A, Kumar P, Tyagi NTN. Synthesis and characterization of sulfamethoxazole derivatives. J Drug Deliv Ther. 2025;15(8):1-8. https://doi.org/10.22270/jddt.v15i8.7302

21. Kumar M, Arya DK, Almujri SS, Chidambaram K, Pandey P, Kumar A, et al. Mulberry silk worm pupae oil and Prussian blue nanoparticle enriched multi-faceted polyvinyl alcohol nanofiber for infectious full thickness skin wound healing. Tissue Engineering and Regenerative Medicine. 2025; 1-22. https://doi.org/10.1007/s13770-025-00751-8 PMid:40974525

22. Srujani KSN, Annapurna, Pawar AKM. Analytical Quality by Design approach in RP-HPLC method development and validation for the determination of Duvelisib. Asian Journal of Pharmaceutical and Clinical Research. 2021;14(2):99-108. https://doi.org/10.22159/ajpcr.2021.v14i2.40181

23. Srujani KSN, Harika, Pawar AKM. RP-HPLC method development and validation for the determination of Pemigatinib using the Design of Experiments approach. Journal of Pharmaceutical Research International. 2020;32(40):26-48. https://doi.org/10.9734/jpri/2020/v32i4031031